

## THE METHOD OF THE TIME-OF-FLIGHT TRIGGER WITH DIGITAL SELECTION OF EVENTS

V.P.Ladygin, P.K.Manyakov, N.M.Piskunov

The method of timing measurements and the realization of the time-of-flight trigger with digital selection using the magnetic spectrometer ALPHA are reported. The decision time of the time-of-flight trigger is  $8 \mu\text{s}$ . High rejection power of the trigger without losses confirms the efficiency of the suggested method. A further development of the digital selection system is discussed.

The investigation has been performed at the Laboratory of High Energies, JINR.

### Метод цифрового отбора событий по времени пролета

В.П.Ладыгин, П.К.Маньяков, Н.М.Пискунов

Представлены результаты по временным измерениям и реализации триггера по времени пролета частиц с цифровым отбором событий на магнитном спектрометре АЛЬФА. Время решения триггера по времени пролета составляет 8 мксек. Полное подавление событий вне выбранного временного интервала без потери статистики свидетельствует об эффективности предложенного метода. Обсуждаются пути дальнейшего улучшения системы цифрового отбора.

Работа выполнена в Лаборатории высоких энергий ОИЯИ.

### 1. Introduction

Particle identification is achieved by measuring the times of flight and momenta of the registered particles. The mass of the particle is determined from the equation:

$$M = p \sqrt{\left(\frac{tc}{L}\right)^2 - 1}, \quad (1)$$

where  $M$  is the mass of the particle;  $p$ , its momentum;  $t$ , the time of flight of the particle over a distance  $L$ , and  $c$  is the speed of light.

Of particular interest is the possibility of discriminating against a specific kind of particles (for example, protons or deuterons) at the trigger level in the study of processes having small cross sections in the presence of a high background rate. As an example of such a situation, Fig.1 shows the time-of-flight spectrum of protons from  $dp$  backward elastic scattering at an angle of  $180^\circ$  and of background inelastic deuterons of the same momentum.

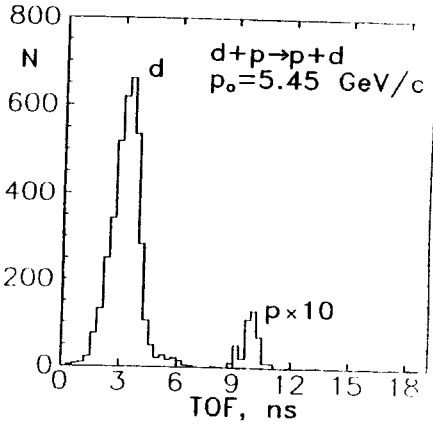


Fig.1. Time-of-flight spectrum of protons from  $dp$  backward elastic scattering at  $180^\circ$  and background inelastic deuterons

The ratio of deuterons to protons is of the order of  $10^3$ , and therefore it is necessary to select protons at the trigger level for efficient data taking.

In the present paper we describe the method of timing measurements and the realization of the time-of-flight trigger with digital selection

using the magnetic spectrometer "ALPHA" with a polarized deuteron beam at the Dubna synchrophasotron.

## 2. Method of Timing Measurements

Two particles with the same momentum but different masses  $m_1$  and  $m_2$  differ in the times of flight over a baseline  $L$ :

$$\Delta T = T_{m_1} - T_{m_2} = \frac{L}{c} \left( \sqrt{1 + \left(\frac{m_1}{p}\right)^2} - \sqrt{1 + \left(\frac{m_2}{p}\right)^2} \right). \quad (2)$$

It is clear that for the identification of particles by their times of flight, it is necessary to increase the baseline  $L$  or to improve significantly the timing resolution of the time-of-flight system.

In modern high energy physics experiments [1—12] the typical difference of the times of flight is of the order of a few ns, and that sets severe demands on the timing resolution of the used detectors and electronics.

There are some main contributions to the resolution of the time-of-flight system [20—21]:

- 1) fluctuations in the time of arrival of photons at the PMT due to the decay time of scintillator light (time dependence of the intensity of a hit in the counter), dispersion of the path length of photons inside the scintillator, the conditions of light collection and so on,
- 2) a timing jitter of the photomultiplier,
- 3) a jitter of the spectrometer track and associated electronics.

Therefore, the timing resolution of the system is:

$$\sigma^2 = \sigma_{sc}^2 + \sigma_{pm}^2 + \sigma_{el}^2, \quad (3)$$

where  $\sigma_{sc}$  is the contribution of the scintillator to the jitter;  $\sigma_{pm}$ , the timing jitter of the photomultiplier;  $\sigma_{ej}$ , the jitter of the electronics.

Achievements in the direction of improving the timing resolution of a scintillator counter are the design of scintillators with a low decay time, better light collection, viewing of the scintillator by two or more PMTs [13—19], use of faster photomultipliers [26], time-walk corrections proportional to the total pulse height of a signal, etc. — all of which make it possible to reach a time resolution of  $\approx 170$  ps [4].

### 3. Realization of the Time-of-Flight Trigger with Digital Selection of Events

To measure the polarization transfer from deuteron to proton, it is necessary to provide both a reliable identification of protons and the possibility to discriminate against inelastic deuterons. A schematic view of the measurements is presented in Fig.2. The slow extracted beam of vector polarized deuterons with an intensity of  $\approx 10^9$  particles per burst is incident on the carbon target  $T_1$  disposed in the focal plane  $F_3$  of the beam line VP1. The momentum of the deuterons varied from 9 to 6 GeV/c. The particles, produced by the interaction of the primary beam with the target  $T_1$ , with a momentum of 4.5 GeV/c, are directed to the target  $T_2$  of the setup ALPHA. Their angles and momenta are measured before and after  $T_2$  by the proportional chambers (PC) of the magnetic spectrometer ALPHA.

The scintillator counters  $S_{t1}$ ,  $S_{t2}$ , and  $S_{t3}$  are used to measure the times of flight of the particles. The counter  $S_{t3}$  was mounted in front of the second target,  $S_{t1}$  and  $S_{t2}$  in the focal plane  $F_4$  of the beam line VP1. The position of

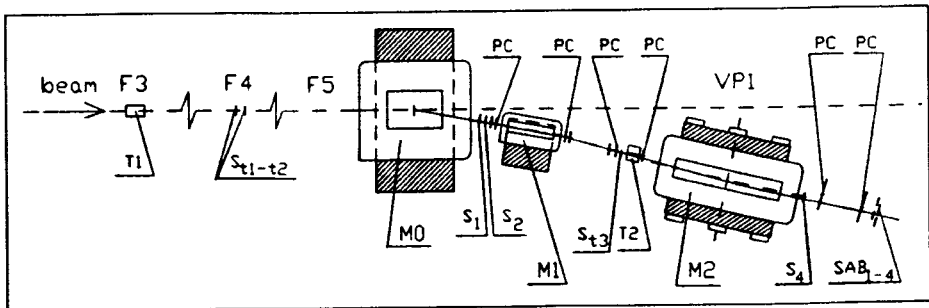


Fig.2. Overview of the magnetic spectrometer ALPHA.  $S_i$  — scintillator counters, PC — proportional chambers,  $M_i$  — magnetic elements,  $T_2$  — second target

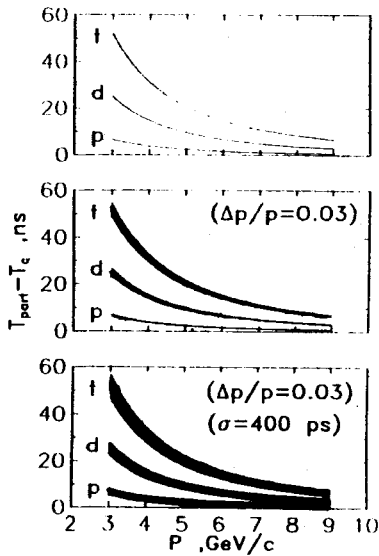


Fig.3. Times of flight of protons, deuterons and tritons over a baseline of 42 m versus their momenta: a) theoretical curves: b) taking into account the momentum acceptance of the magnetic spectrometer  $\Delta p/p = 0.03$ ; c) taking into account  $\Delta p/p = 0.03$  and the internal resolution of the TOF-system ( $\sigma \cong 400$  ps)

b) the counters at focus  $F_4$  allows one to minimize the influence of the material of the counters on beam parameters. The distance between  $S_{t1}$ , ( $S_{t2}$ ), and  $S_{t3}$  was 42 m. The difference of the times of flight over this baseline for deuterons and protons with momentum  $P_0 = 4.5$  GeV/c is

$$t_d - t_p = 8.67 \text{ ns} \text{ (Fig.3a).}$$

Taking into account the momentum acceptance of the magnetic spectrometer  $\Delta p/p$ , we select particles having the time of flight over the time interval:

$$\frac{\Delta t}{t_0} = - \left( \frac{1}{1 + p^2/m^2} \right) \frac{\Delta p}{p_0}, \quad (4)$$

(see Fig.3b).

The Amperex XP2020 [25] photomultipliers are used at one end of the scintillators of each counter. The dimensions of the scintillators are  $100 \times 100 \times 5 \text{ mm}^3$  for  $S_{t3}$  and  $150 \times 60 \times 5 \text{ mm}^3$  for  $S_{t1}$  and  $S_{t2}$ .

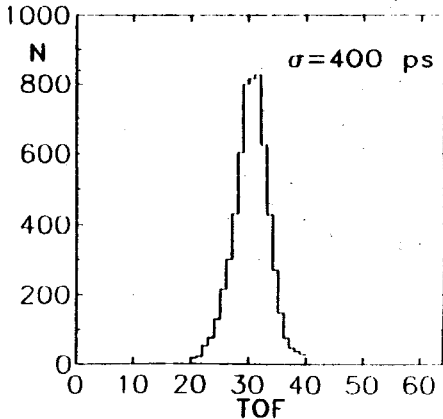


Fig. 4. Internal resolution of the time of flight system

The curves describing the timing resolution of the TOF-system for a baseline of 42 m, the momentum acceptance of the magnetic spectrometer of  $\Delta p/p = 0.03$  and an intrinsic resolution of  $\cong 400$  ps versus the momentum of the registered particle are presented in Fig.3c. The internal resolution of the TOF-system obtained from  $S_{t1}$  and  $S_{t2}$  information is  $\cong 400$  ps (Fig.4).

The timing jitter of the electronics

$\sigma_{el}$  is  $\cong 150$  ps; the jitter of the photomultipliers  $\sigma_{pm} \cong 260+300$  ps and the intrinsic resolution of the counters  $S_{t1}$ ,  $S_{t2}$ , and  $S_{t3}$ , about  $300 + 350$  ps.

The coincidence of the counters  $S_1$ ,  $S_2$ ,  $S_{t3}$ ,  $S_4$ , and  $\sum_{i=1}^4 SAB_i$  is used as a first level trigger. The jitter of a trigger signal is  $\cong 2$  ns. This does not allow one to establish the time-of-flight trigger by the analog method nor by using a coincidence circuit with short discrimination times [22—24,27] under the conditions of our measurements (Fig.3c).

The idea of the time-of-flight trigger is based on the use of a series of reference frequency signals of the time-to-digital converter (TDC). The schematic diagram of the time-of-flight trigger with digital selection and the timing diagrams explaining its operation are presented in Figs.5 and 6, respectively.

The choice of  $S_{t3}$  as a start counter decreases significantly the number of accidental starts of the system because, firstly, the typical rates are

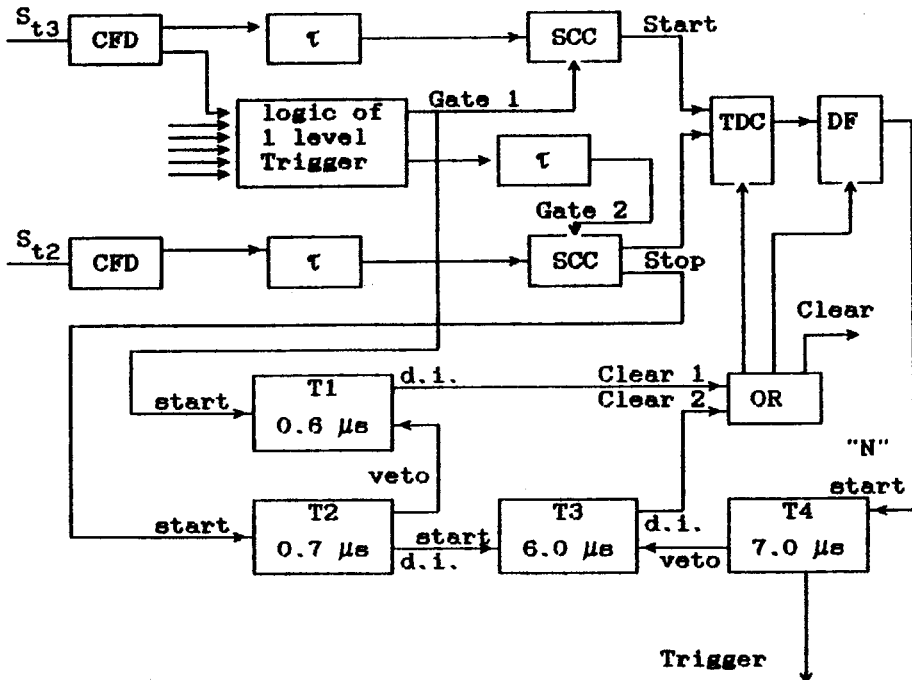


Fig.5. Organization of the time of flight trigger with digital selection. CFD — constant fraction discriminators, SCC — strobed coincidence circuits,  $T_i$  — timers, TDC — time to digital converter, DF — frequency divider,  $\tau$  — delays

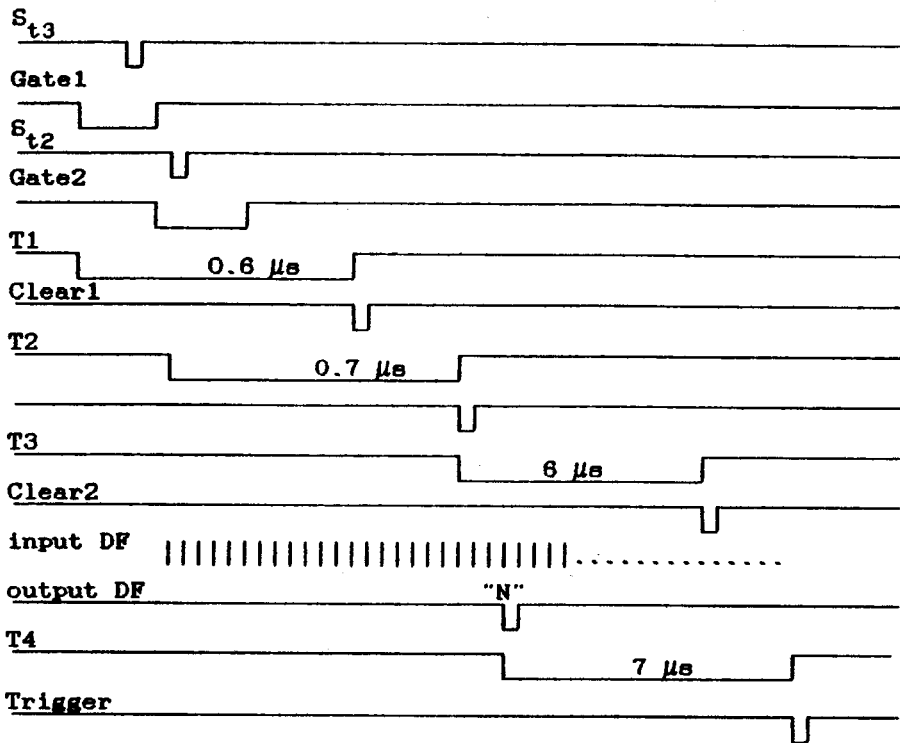


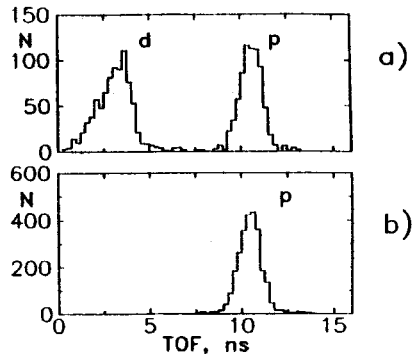
Fig.6. Time diagram of the time of flight trigger operation

$2 \cdot 10^3$  for  $S_{t3}$  and  $3 \cdot 10^5$  for  $S_{t2}(S_{t1})$  per burst (400 ms) and, secondly,  $S_{t3}$  is included in the logic of the first level trigger.

Signals from the counters  $S_{t3}$  and  $S_{t2}$  are fed to the inputs of the constant fraction discriminators (CFD). The CFD output signal occurs independently of pulse height  $U_{in}$  and is created when the incoming pulse reaches  $\alpha U_{in}$ , where  $\alpha < 1$ . Experience with time-of-flight systems shows that a better time resolution for the scintillator detectors is obtained providing  $\alpha \cong 0.05 \pm 0.2$  [30]. We are using  $\alpha = 0.2$ . The thresholds of the CFDs are  $\cong 60 \text{ mV}$ .

The shaped signals, having a duration of  $\cong 30 \text{ ns}$  are passed through the coincidence circuits (SCC) strobed by a first level trigger signal (Gate 1 and Gate 2). The strobe duration is  $\cong 85 \text{ ns}$ . This is determined by the time spread of stopping signals from deuterons and protons and by the duration of the CDF output signals.

Fig.7. Time of flight spectra of secondary particles:  
a) without selection; b) with time of flight selection



Event selection according to the time of flight was done in 2 stages. At the first stage the mandatory presence of the signal  $S_{t2}$  is required. In the absence of this signal, «Clear 1» is generated to clear information in the CAMAC crates and to reenable the data acquisition system. The decision time is  $0.6 \mu\text{s}$ .

The type of particle is identified by the presence of a signal from the counter  $S_{t2}$ . For this purpose a series of reference signals with a frequency of 20 MHz taken from the TDC circuit is fed to the input of the frequency divider (DF), controlled either manually or by a CAMAC-bus.

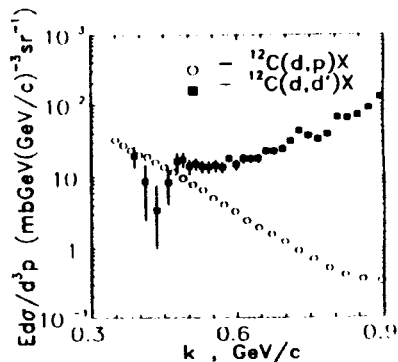
If the number of reference signals is larger than the set «N», the DF generates a signal which indicates that the time interval ( $T_{\text{stop}} - T_{\text{start}}$ ) is longer than  $N \cdot 0.125 \text{ ns}$ . In this case data-taking is initiated. When there is no DF signal, «Clear 2» is generated to clear information in the CAMAC crates and to reenable the data acquisition system. The total decision time of the trigger is  $\approx 8 \mu\text{s}$ .

The time of flight spectra ( $k \approx 420 \text{ MeV}/c$ ) with and without time of flight selection are presented in Fig.7. The ratio of inelastic deuterons from the reaction  $^{12}\text{C}(d,d')X$  to protons from the reaction  $^{12}\text{C}(d,p)X$  corresponds to the expected one [28—29]. The differential cross sections of these reactions versus the light-cone variable  $k$  are shown in Fig.8.

The total suppression of unwanted particle, the high rejection power of the trigger without losses confirm the efficiency of the suggested method of the time-of-flight trigger. Undoubtedly, advantages of the proposed method are also the possibility of computer control, the dialog regime included, and relative simplicity in tuning (in comparison with other methods of trigger realization) which is very essential in the analysis of rare processes.

To achieve the above method, standard electronics circuits made at the

Fig.8. Data on the differential cross sections from the reactions  $^{12}\text{C}(d,d')X$  and  $^{12}\text{C}(d,p)X$  versus the light-cone variable  $k(k \approx 420 \text{ MeV}/c)$



Laboratory of High Energies are used. A further development of the digital selection system is possible by decreasing the duration of signals from CDF from 30 ns to 5 ns and the strobe duration from 85 ns to 30 ns, respectively, and by increasing the frequency of reference signals approximately by a factor of 10.

The authors would like to express their thankfulness to I.M.Sitnik, E.A.Strokovsky and L.Penchev for stimulation of interest in this work and constant help at all its stages. Also, the authors would like to thank N.S.Moroz for the given scintillator counters; Yu.A.Kozhevnikov, I.G.Zarubina, Yu.S.Anisimov, V.M.Grebenyuk for their help in the present work.

## References

1. Azhgirey L.S. et al. — JINR Preprint P1-85-749, Dubna, 1985.
2. Bunjatov S.L. et al. — PTE, 1978, N1, p.23.
3. Banerjee S. et al. — NIM, 1988, A269, p.121.
4. Brown J.S. et al. — NIM, 1984, 221, p.504.
5. Bell K.W. et al. — NIM, 1981, 179, p.27.
6. Antipov Y.M. et al. — NIM, 1989, A274, p.452.
7. Benlloch J.M. et al. — NIM, 1990, A290, p.327.
8. Basile M. et al. — NIM, 1981, 179, p.447.
9. Chi peng Cheng et al. — NIM, 1986, A252, p.67.
10. Agostini G.D. et al. — NIM, 1984, 219, p.495.
11. Heller R. et al — NIM, 1985, A235, p.26.
12. Braunschweig W. et al. — NIM, 1976, 134, p.261.
13. Agostini G.D. et al. — NIM, 1981, 185, p.49.
14. Bressani T. et al. — NIM, 1984, 221, p.355.
15. Binon F. et al. — NIM, 1978, 153, p.409.
16. Kobayashi T. et al. — NIM, 1990, A287, p.389.
17. Benlloch J.M. et al. — NIM, 1990, A292, p.319.
18. Tanimori T. et al — NIM, 1983, 216, p.57.
19. Abramov B.M. et al. — PTE, 1979, N5, p.52.
20. Milliken B. et al. — Contribution to the Workshop on Scintillating Fiber Detector Development for the SSC, Fermilab, November 1988.
21. Moszynski M. et al. — NIM, 1979, 158, p.1.
22. Borejko V.F. et al. — JINR Preprint 13-86-362, Dubna, 1986.
23. Grebenyuk V.M. et al. — JINR Preprint 13-87-846, Dubna, 1987.
24. Azhgirey L.S. et al. — JINR Preprint 13-88-437, Dubna, 1988.
25. Philips, DATA Handbook, 1985.
26. Lo C.C. et al. — IEEE Trans. on Nucl. Sci., 1981, NS-28, p.659.



27. Kozhevnikov Ju.A. et al. — JINR Preprint 13-88-627, Dubna, 1988.
28. Ableev V.G. et al. — JINR Preprint 1-82-278, Dubna, 1982.
29. Ableev V.G. et al. — JINR Rapid Communications, No.1 [52 ], Dubna, 1992, p.10.
30. Grigorjev V.A. et al. — Electronic Methods in Nuclear Physics Experiment. M.: Energoatomizdat, 1988, p.158.

Received on January 27, 1993.